# Rapidly rotating self-gravitating Boussinesq fluid: A nonspherical model of motionless stable stratification

Dali Kong *
*CAS Key Laboratory of Planetary Sciences, Shanghai Astronomical Observatory, Chinese Academy of Sciences, Shanghai, 200030, China*

(Received 6 February 2022; accepted 29 June 2022; published 15 July 2022)

Spherical approximation is often adopted in modeling planetary and stellar fluid dynamics, which implicitly assumes the rotational flattening effect is small. This simplification, to the leading order of the basic reference state, makes gravity, pressure, chemical, and thermal variables only depend on the radial coordinate. However, a rotating and self-gravitating fluid body is necessarily nonspherical. In order to represent fundamental mechanical equilibrium and thermal state of rapidly rotating planets or stars, where rotational flattening is not to be neglected, we construct a nonspherical, stably stratified Boussinesq fluid model of uniform rotation. Closed-form gravity and temperature formulations of the basic reference state are derived in terms of oblate spheroidal coordinates. The key emphasis of this paper is that the uniformly heated model is mathematically confirmed to be motionless in the corotating frame of reference. Based on this hydrostatic model of rotating stable stratification, we show that although treating the centrifugal terms within a spherical geometry context is convenient, it can lead to incorrect flows. The neglected terms produced by the oblateness are of the same order as the baroclinic terms included, and can indeed cancel them out in some circumstances. This paper proposes a foundation for the analysis of thermally driven flows in nonspherical geometries, which will be carried on in a series of future papers.

DOI: 10.1103/PhysRevFluids.7.074803

## I. INTRODUCTION

Flow and turbulence in a celestial body play a crucial role in chemical mixing, thermal evolution, and magnetic field generation. It is widely accepted that buoyancy force in unstably stratified convective zones can drive differential rotation, meridional circulation, nonaxisymmetric flow, and turbulence that transport heat and power planetary and stellar dynamos in uniformly rotating planets and stars. The problem of thermal convections, in which the radial buoyancy force plays a major dynamical role, has been formulated and modeled in spheres and spherical shells by many authors [1–13, e.g.]. However, there are also examples of stable stratification. The radiative region in a star is a typical thermally stable stratification. In a gaseous giant planet, there could be a helium-hydrogen immiscible layer also being stably stratified because of compositional separation [14]. In contrast to an unstably stratified convective zone, fluid motions in stably stratified zones are not driven by radial buoyancy force but could be caused by baroclinicity that is sensitive to thermal and geometric conditions. As a result, there are fundamental differences in modeling the two distinct categories of dynamics.

Von Zeipel theorem [15] is concerned with whether motionless stable stratification exists in a uniformly rotating star. Von Zeipel reached a general conclusion that an equilibrium solution of a

*dkong@shao.ac.cn

 

rotating radiative star would be possible only if

$$\varepsilon = C\left(1 - \frac{\Omega^2}{2\pi G\rho}\right), \tag{1}$$

in which $\varepsilon$ is the rate of heat generation per unit mass, $C$ is a constant, $\Omega$ is the solid-body rotation rate of the star, $G$ is the universal gravitational constant and $\rho$ is the mass density [15,16]. Equivalently, if the heat source distribution in a rotating stably stratified region does not obey Eq. (1), fluid will not be at rest in the corotating frame of reference. Because the condition suggested by Eq. (1) is not physically sound for stellar interior, Eddington in 1925 [17] first proposed there would not be hydrostatic equilibrium in a rotating radiative star. Along this line, by far, there have been lots of relevant analyses on rotationally induced baroclinicity, meridional circulations, and differential rotations [18–24, e.g.].

More recently, Rieutord [25] developed a three-dimensional (3D) Boussinesq model of the radiative envelope of rotating stars, in which rotational baroclinic flows are computed in spherical geometry. Simitev and Busse [26,27] reported a 3D anelastic dynamo model in which magnetic field is generated and sustained by rotational baroclinic flows that are computed in a stably stratified spherical shell. In these models the basic state temperature is a function of radius $r$ only, but because the centrifugal force is not in the radial direction, it is impossible to balance the centrifugal buoyancy with uniform rotation by pressure, so either a circulation is driven or there must be a differential rotation that adjusts the centrifugal buoyancy so that it can balance a pressure gradient. In Refs. [25–27] the differential rotation required is computed using the thermal wind equation in spherical geometry. This nonzero differential rotation is found even in the uniform heating case studied by von Zeipel, which is slightly surprising as von Zeipel showed this was the only case in which no differential rotation is required to get hydrostatic equilibrium. This suggests that if the problem is studied in oblate geometry rather than spherical geometry, the changes in the thermal wind balance arising from the oblate geometry exactly balance the terms arising from the nonzero curl of the centrifugal buoyancy. With more general heat sources than uniform heating or cooling, these effects will no longer cancel each other exactly, and differential rotation will occur. However, it is apparent that the errors made by neglecting the oblateness are of the same order of magnitude as those arising from the nonzero curl of the centrifugal buoyancy, so that unfortunately the results obtained from the spherical geometry approach may well be unreliable.

Reconsidering the problem of stable stratification is also for the purpose of studying the onset of thermal instability. In order to carry out linear or nonlinear analysis of thermal instability, it is desirable to first have a basic reference state on top of which convective variables can be regarded as small perturbation [28]. Such a basic reference state is commonly stably stratified. Spherical approximation of a rotating self-gravitating fluid, to the leading order of the basic reference state, makes gravity, pressure, chemical, and thermal variables only depend on the radial coordinate. It simplifies perturbation analysis and facilitates numerical modeling of convective motions. If the geometrical flattening due to rotation is taken into account, the basic state will be much more complicated. In this paper, we derive the first closed-form solution of a nonspherical basic reference state in terms of oblate spheroidal coordinates and confirm motionless equilibrium exists in the corotating frame of reference. The Boussinesq approximation is adopted, which is widely applied in Earth and planetary contexts. The shape of a self-gravitating incompressible fluid that is rotating uniformly can be described by an oblate spheroid [29]. For a fluid of internally differentiated density, the rotational equilibrium figure will no longer be perfectly spheroidal. But the departure from an oblate spheroid will be typically very small. For example, for Jupiter's rotation rate and density stratification, such nonspheroidal undulation on the 1-bar surface is no more than 0.01% relative to the best-fit reference spheroid [30]. Therefore, an oblate spheroid also can be a good first approximation to a rapidly rotating gaseous body. Based on the hydrostatic non-spherical basic reference state of gravity and temperature, thermal instability of rotating Boussinesq fluid can be

discussed in the ensuing papers. It will be interesting to understand how the symmetry, onset, and structure of convective flow depend on nonsphericity.

In what follows, rotationally induced baroclinic torque in a spherical Boussinesq fluid model is necessarily reviewed in Sec. II for a comparison purpose. Section III presents the mechanical and thermal solution, as the basic reference state below the onset of convection, in a rapidly rotating oblate spheroid. It is convincingly demonstrated that baroclinicity ought to vanish, which is consistent with the von Zeipel theorem. The baroclinicity that appears in spherical models reported in Refs. [25–27] is not physically sound. A numerical verification is presented in Sec. IV, followed by extra discussions in Sec. V.

## II. ROTATIONAL BAROCLINICITY IN A SPHERICAL MODEL OF STABLE STRATIFICATION

Consider first a stably stratified, nonrotating sphere under the Boussinesq approximation which has been widely used in models of astrophysical stable stratification zones [1,25]. The Boussinesq fluid is confined within a sphere of radius $R_e$ with constant thermal expansion $\alpha$, thermal diffusivity $\kappa$ and kinematic viscosity $\nu$, whose density $\rho$ is described by $\rho = \rho_0(1 - \alpha T)$ where $\rho_0$ is the density at a reference temperature $T = 0$. It is assumed that fluid rotates uniformly with constant angular velocity $\boldsymbol{\Omega} = \hat{\boldsymbol{z}}\Omega$, where $\hat{\boldsymbol{z}}$ denotes the unit vector, and is confined within a spherical bounding surface $\mathcal{S}(r = R_e)$ marked by the reference temperature $T = 0$. Analyses are to be carried out using spherical coordinates $(0 \leqslant r \leqslant R_e, 0 \leqslant \theta \leqslant \pi, 0 \leqslant \phi < 2\pi)$. The mechanical and thermal equilibrium of the stably stratified sphere is governed by the equations

$$-\frac{dp_0(r)}{dr} + \rho_0(r)\boldsymbol{g}_0(r) = \boldsymbol{0},$$
$$\frac{1}{r^2}\frac{d}{dr}\left(r^2\frac{dT_0(r)}{dr}\right) - \beta = 0,$$

where the gravity

$$\boldsymbol{g}_0 = -(4\pi G\rho_0/3)\boldsymbol{r}, \tag{2}$$

and $-\beta$ denotes uniform heat sink source with $\beta > 0$. $\boldsymbol{r}$ is the position vector. The pressure $p_0$ is a passive variable. Usually the gravity factor is denoted by $\gamma = 4\pi G\rho_0/3$. The equilibrium temperature in the sphere can be solved as

$$T_0(r) = \frac{\beta}{6}\left(r^2 - R_e^2\right). \tag{3}$$

In the corotating frame, flow is driven by baroclinic torque, which can be shown by perturbation analysis. Considering the flow inducing perturbations in pressure, density, and temperature as

$$p = p_0(r) + \tilde{p}(r,\theta),\ \ \rho = \rho_0(r) + \tilde{\rho}(r,\theta),\ \ T = T_0(r) + \tilde{T}(r,\theta),$$

and using the Boussinesq approximation, we find the governing equations for perturbation variables:

$$\left[\frac{\partial \boldsymbol{u}}{\partial t} + \boldsymbol{u}\cdot\boldsymbol{\nabla}\boldsymbol{u} + 2\boldsymbol{\Omega}\times\boldsymbol{u}\right] = -\frac{1}{\rho_0(r)}\boldsymbol{\nabla}\tilde{p} + \alpha[\boldsymbol{\Omega}\times(\boldsymbol{\Omega}\times\boldsymbol{r}) - \boldsymbol{g}_0(r)]\tilde{T} + \nu\nabla^2\boldsymbol{u}$$
$$+ \alpha[\boldsymbol{\Omega}\times(\boldsymbol{\Omega}\times\boldsymbol{r}) - \boldsymbol{g}_0(r)]T_0(r),$$
$$\boldsymbol{\nabla}\cdot\boldsymbol{u} = 0,$$
$$\frac{\partial\tilde{T}}{\partial t} + \boldsymbol{u}\cdot\boldsymbol{\nabla}[T_0(r) + \tilde{T}] = \kappa\nabla^2\tilde{T}. \tag{4}$$

Taking the curl of Eq. (4) arrives at

$$\nabla \times \left[ \frac{\partial \boldsymbol{u}}{\partial t} + \boldsymbol{u} \cdot \nabla \boldsymbol{u} + 2\boldsymbol{\Omega} \times \boldsymbol{u} + \alpha(\Omega^2 s\hat{\boldsymbol{s}} + \boldsymbol{g}_0)\tilde{T} - \nu\nabla^2 \boldsymbol{u} \right] = -\frac{\alpha\beta\Omega^2}{3} r^2 \sin\theta\cos\theta\hat{\boldsymbol{\phi}}, \\ \stackrel{\text{def}}{=} \boldsymbol{\mathcal{L}}_{\text{sphere}}, \tag{5}$$

where $s$ is the distance from the rotation axis and $\hat{\boldsymbol{s}}$ is the cylindrical unit radial vector. Equation (5) is exactly equivalent to Eq. (3) of [25] if $Q$ is taken to be constant therein. The torque $\boldsymbol{\mathcal{L}}_{\text{sphere}}$ is connected with the centrifugal force $\boldsymbol{\Omega} \times (\boldsymbol{\Omega} \times \boldsymbol{r})$, without which, namely $\boldsymbol{\Omega} = \boldsymbol{0}$, both the baroclinicity and the torque will vanish. It looks as if flow is always driven by the torque as long as rotation is present.

A key question is whether such flow is physically inevitable or only a result of the model setting. Note that because of the choice of the spherical geometry, the isopycnals and isobars of the obtained model are all spherical, but the equipotential levels depart from sphericity due to the centrifugal force. To the leading order, mechanically speaking, such model configuration in fact cannot represent a uniformly rotating equilibrium. Also, because the spherical isothermal surfaces are also misaligned with the nonspherical equipotential surfaces, it is impossible to balance the centrifugal buoyancy by pressure. The inconsistency suggests that the spherical approximation needs to be reconsidered.

## III. A NONSPHERICAL MODEL OF ROTATING STABLE STRATIFICATION AND ITS IMPLICATIONS

The shape of a rotationally distorted self-gravitating fluid under the Boussinesq approximation is described by oblate spheroid [29] characterized by its eccentricity $e$ defined as $e = \sqrt{R_e^2 - R_p^2}/R_e$, where $0 < e < 1$ and $R_e$ and $R_p$ are the equatorial and polar radius of an oblate spheroid, respectively. In the mathematical analysis, it is convenient to introduce oblate spheroidal coordinates [31] ($\xi \geqslant 0, -1 \leqslant \eta \leqslant 1, 0 \leqslant \phi < 2\pi$) linked to Cartesian coordinates via

$$x = R_e e\sqrt{(1+\xi^2)(1-\eta^2)}\cos\phi,$$
$$y = R_e e\sqrt{(1+\xi^2)(1-\eta^2)}\sin\phi,$$
$$z = R_e e\xi\eta.$$

With the help of the above spheroidal coordinates, the free space Green's function

$$G_{\text{free}}(\xi,\eta,\phi;\xi',\eta',\phi') = -\frac{1}{4\pi}\frac{1}{|\boldsymbol{r}-\boldsymbol{r}'|} \\ = -\frac{1}{4\pi R_e e}\sum_{\ell=0}^{\infty}\sum_{m=0}^{\ell} \mathrm{i}(2-\delta_{0m})(-1)^m(2\ell+1) \\ \times\left[\frac{(\ell-m)!}{(\ell+m)!}\right]^2 P_\ell^m(\eta)P_\ell^m(\eta')\cos m(\phi-\phi') \\ \times\begin{cases} P_\ell^m(\mathrm{i}\xi)Q_\ell^m(\mathrm{i}\xi'), & \xi < \xi', \\ P_\ell^m(\mathrm{i}\xi')Q_\ell^m(\mathrm{i}\xi), & \xi > \xi', \end{cases}$$

and the Green's function satisfying the homogeneous boundary condition on the spheroidal bounding surface $\mathcal{S}(\xi = \xi_o = \sqrt{1/e^2 - 1})$

$$
\begin{aligned}
&G_{\text{homo}}(\xi, \eta, \phi; \xi', \eta', \phi') \\
&= -\frac{1}{4\pi R_e e} \sum_{\ell=0}^{\infty} \sum_{m=0}^{\ell} \mathrm{i}(2 - \delta_{0m})(-1)^m (2\ell + 1) \left[ \frac{(\ell - m)!}{(\ell + m)!} \right]^2 P_\ell^m(\eta) P_\ell^m(\eta') \cos m(\phi - \phi') \\
&\times \begin{cases} P_\ell^m(\mathrm{i}\xi) Q_\ell^m(\mathrm{i}\xi') - \dfrac{Q_\ell^m(\mathrm{i}\xi_o)}{P_\ell^m(\mathrm{i}\xi_o)} P_\ell^m(\mathrm{i}\xi) P_\ell^m(\mathrm{i}\xi'), & \xi < \xi', \\ P_\ell^m(\mathrm{i}\xi') Q_\ell^m(\mathrm{i}\xi) - \dfrac{Q_\ell^m(\mathrm{i}\xi_o)}{P_\ell^m(\mathrm{i}\xi_o)} P_\ell^m(\mathrm{i}\xi') P_\ell^m(\mathrm{i}\xi), & \xi > \xi', \end{cases}
\end{aligned}
$$

in which $\mathrm{i} = \sqrt{-1}$, $\delta$ denotes the Kronecker symbol, $P_\ell^m(\eta)$ are Legendre polynomials, $P_\ell^m(\mathrm{i}\xi)$, $Q_\ell^m(\mathrm{i}\xi)$ are Legendre functions of imaginary argument, the rotational equilibrium equations

$$\rho_0 \boldsymbol{\Omega} \times (\boldsymbol{\Omega} \times \boldsymbol{r}) = -\nabla p_0(\boldsymbol{r}) + \rho_0 \boldsymbol{g}_0(\boldsymbol{r}), \tag{6}$$

$$\boldsymbol{g}_0(\boldsymbol{r}) = -\nabla V_g(\boldsymbol{r}), \tag{7}$$

$$\nabla^2 V_g(\boldsymbol{r}) = 4\pi G \rho_0, \tag{8}$$

$$\nabla^2 T_0(\boldsymbol{r}) - \beta = 0, \tag{9}$$

subject to the boundary conditions on the spheroidal bounding surface

$$
\begin{aligned}
&p_0|_{\mathcal{S}} = \text{constant}, \\
&T_0|_{\mathcal{S}} = 0, \\
&V_g|_{\xi \to \infty} = 0, \\
&\left( V_g - \frac{1}{2} |\boldsymbol{\Omega} \times \boldsymbol{r}|^2 \right)_{\mathcal{S}} = \text{constant},
\end{aligned}
$$

are solved by

$$\hat{\boldsymbol{\xi}} \cdot \boldsymbol{g}_0 = \frac{4\pi G \rho_0 R_e}{3} \frac{3\xi}{2e^2} \sqrt{\frac{1 + \xi^2}{\xi^2 + \eta^2}} [e - 3e\eta^2 - e^3(1 - \eta^2) + \sqrt{1 - e^2}(3\eta^2 - 1) \sin^{-1} e], \tag{10}$$

$$\hat{\boldsymbol{\eta}} \cdot \boldsymbol{g}_0 = \frac{4\pi G \rho_0 R_e}{3} \frac{3\eta}{2e^2} \sqrt{\frac{1 - \eta^2}{\xi^2 + \eta^2}} [-e + e^3 - e\xi^2(3 - e^2) + \sqrt{1 - e^2}(3\xi^2 + 1) \sin^{-1} e], \tag{11}$$

$$\frac{2Fr}{3} = \frac{\sqrt{1 - e^2}}{e^3}(3 - 2e^2) \sin^{-1} e - \frac{3(1 - e^2)}{e^2}. \tag{12}$$

$$T_0 = \beta R_e^2 \frac{[1 - e^2(1 - \eta^2)][1 - e^2(1 + \xi^2)]}{4e^2 - 6}. \tag{13}$$

Note that in the nonrotating limit, $\Omega \to 0$ hence $e \to 0, e\xi \to r/R_e, \eta \to \cos\theta$, Eq. (10)–(13) return to Eqs. (2) and (3). Equation (12) is the classical Maclaurin spheroid relation [1,29] that connects the spheroidal figure of a self-gravitating homogeneous fluid to its rotational parameter $Fr = 3\Omega^2/(4\pi G \rho_0)$. Equations (10)–(12) mark a mechanical equilibrium. Equation (13) establishes the thermal state that is confined by such equilibrium.

It is tempting to think that when the strength of the sink source $-\beta$ becomes sufficiently strong, the corresponding baroclinic effect would drive a substantial flow $\boldsymbol{u}$, similar to the problem demonstrated in Sec. II. The problem of self-consistent baroclinically driven flow in a uniformly

rotating oblate spheroid is governed by the dimensional equations that are defined in the oblate spheroidal domain enclosed by the bounding surface $\mathcal{S}$ of eccentricity $e$:

$$\left[\frac{\partial \boldsymbol{u}}{\partial t}+\boldsymbol{u}\cdot\boldsymbol{\nabla}\boldsymbol{u}+2\boldsymbol{\Omega}\times\boldsymbol{u}\right]=-\frac{1}{\rho_0}\boldsymbol{\nabla}\tilde{p}+\alpha[\boldsymbol{\Omega}\times(\boldsymbol{\Omega}\times\boldsymbol{r})-\boldsymbol{g}_0(\xi,\eta)]\tilde{T}+\nu\nabla^2\boldsymbol{u}$$
$$+\alpha[\boldsymbol{\Omega}\times(\boldsymbol{\Omega}\times\boldsymbol{r})-\boldsymbol{g}_0(\xi,\eta)]T_0(\xi,\eta), \tag{14}$$

$$\boldsymbol{\nabla}\cdot\boldsymbol{u}=0, \tag{15}$$

$$\frac{\partial\tilde{T}}{\partial t}+\boldsymbol{u}\cdot\boldsymbol{\nabla}(T_0(\xi,\eta)+\tilde{T})=\kappa\nabla^2\tilde{T}. \tag{16}$$

Similar to Eq. (5), taking the curl of Eq. (14) arrives at the mathematical form of rotationally induced baroclinic torque

$$\begin{aligned}\boldsymbol{\nabla}\times&\left[\frac{\partial\boldsymbol{u}}{\partial t}+\boldsymbol{u}\cdot\boldsymbol{\nabla}\boldsymbol{u}+2\boldsymbol{\Omega}\times\boldsymbol{u}+\alpha(\Omega^2 s\hat{\boldsymbol{s}}+\boldsymbol{g}_0(\xi,\eta))\tilde{T}-\nu\nabla^2\boldsymbol{u}\right]\\
&=\mathcal{L}(\xi,\eta;e)\hat{\boldsymbol{\phi}}\\
&=-\alpha\beta\gamma R_e^2\frac{3}{6-4e^2}\frac{\xi\eta\sqrt{(1+\xi^2)(1-\eta^2)}}{\xi^2+\eta^2}\\
&\quad\times\left\{[1-e^2(1-\eta^2)]\left[(1+3\xi^2)G(e)+(1+\xi^2)e^2\left(\frac{2Fr}{3}-1\right)\right]\right.\\
&\quad\left.-[1-e^2(1+\xi^2)]\left[(1-3\eta^2)G(e)+(1-\eta^2)e^2\left(\frac{2Fr}{3}-1\right)\right]\right\}\hat{\boldsymbol{\phi}},\end{aligned} \tag{17}$$

where $G(e)=1-\frac{\sqrt{1-e^2}}{e}\sin^{-1}e$.

Although Eq. (17) looks complicated, it can be better understood via its dimensionless volumetric mean

$$\begin{aligned}\langle\mathcal{L}\rangle&=\sqrt{\frac{1}{V}\int_V\left|\frac{\mathcal{L}}{\alpha\beta\gamma R_e^2}\right|^2\mathrm{d}V}\\
&=\sqrt{\frac{3}{4\pi\sqrt{1-e^2}}\int_0^{2\pi}\int_{-1}^{1}\int_0^{\xi_o}\left|\frac{\mathcal{L}(\xi,\eta;e)}{\alpha\beta\gamma R_e^2}\right|^2\cdot e^3(\xi^2+\eta^2)\mathrm{d}\xi\,\mathrm{d}\eta\mathrm{d}\phi},\\
&=\frac{3\sqrt{1-e^2}}{\sqrt{70}(3-2e^2)}\left|\frac{2Fr}{3}-\left[\frac{\sqrt{1-e^2}}{e^3}(3-2e^2)\sin^{-1}e-\frac{3(1-e^2)}{e^2}\right]\right|.\end{aligned} \tag{18}$$

Equation (12), which establishes $e=e(Fr)$, apparently leads to $\langle\mathcal{L}\rangle=0$ and hence strongly implies

$$\mathcal{L}(\xi,\eta;e=e(Fr))=0 \tag{19}$$

for any $0\leqslant\xi\leqslant\xi_o$ and $-1\leqslant\eta\leqslant1$. Mathematically, it means that the motionless state (the flow velocity $\boldsymbol{u}=\boldsymbol{0}$ everywhere in the rotating frame of reference) represent a solution to the governing equations (14)–(16) in a stably stratified, rotating spheroid for any parameters of nonspherical models when $Fr>0$ and $\beta>0$, as long as the eccentricity $e$ of the bounding surface is specifically determined by the Maclaurin spheroid relation. Physically speaking, the source of baroclinicity to do with the centrifugal force $\boldsymbol{\Omega}\times(\boldsymbol{\Omega}\times\boldsymbol{r})$ vanishes in nonspherical geometry when the mechanical equilibrium condition is everywhere reached, including on the bounding surface $\mathcal{S}$. Therefore hydrostatic equilibrium is permitted in the corotating frame of reference.

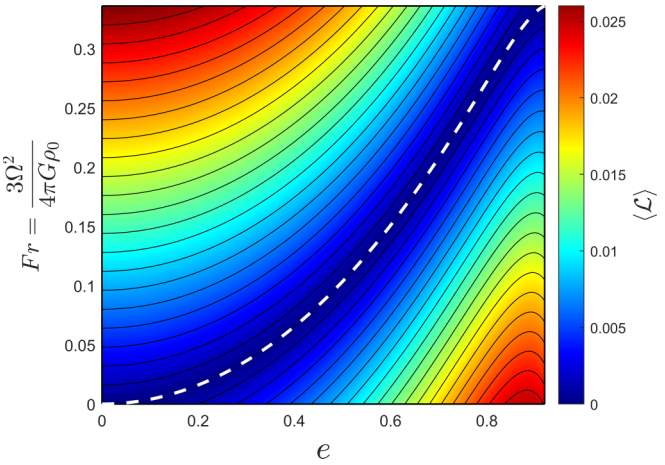


FIG. 1. The RMS torque in oblate spheroidal geometries. The horizontal axis represents the eccentricity $e$ of the outer spheroidal boundary. The vertical axis represents the rotational parameter $Fr$. The color bar shows the size of $\langle \mathcal{L} \rangle$ computed from Eq. (18). Black solid lines depict the contours of $\langle \mathcal{L} \rangle$. The white dashed line indicates the zero-torque curve, which exactly coincides with the Maclaurin spheroid relation as Eq. (12).

In fact, it is not surprising finding that the stable stratification is motionless because von Zeipel theorem [15,16] has already indicated it. In our nonspherical Boussinesq model, the condition Eq. (1) is obeyed. And also, the fundamental hypothesis (the nature of the fluid being constant over every level surface) is also true as density, pressure, thermal, and potential level surfaces all coincide throughout the whole nonspherical fluid domain.

On the other hand, the baroclinicity that appears in the spherical model of rotating stable stratification (see Sec. II) can be better understood. Note that

$$\mathcal{L}(\xi, \eta; e \neq e(Fr)) \neq 0 \tag{20}$$

as also illustrated in Fig. 1. If spherical approximation is adopted, $Fr \neq 0$ but $e \to 0$, $e\xi R_e \to r$, $\eta \to \cos\theta$, it can be shown that

$$\mathcal{L}(\xi, \eta; e \to 0 \neq e(Fr))\hat{\boldsymbol{\phi}} \to \boldsymbol{\mathcal{L}}_{\text{sphere}}.$$

As a matter of fact, the relation $e = e(Fr)$ is equivalent to the fundamental hypothesis of the von Zeipel theorem [15]. In the spherical model of a rotating stably stratified Boussinesq fluid [25], isopycnals and isotherms differ from isobars, giving rise to baroclinicity. As a result, although it seems that Eq. (1) is satisfied, fluid motion yet becomes necessary. But, obviously, the baroclinicity and flow are not physical at all but a pure consequence of the choice of spherical approximation.

The above discussion is presented for a Boussinesq fluid model, which is the primary concern of this paper. Simitev and Busse [26,27] reported a spherical shell gaseous model that is stably stratified and close to an adiabatic state. In their model, the rotationally induced baroclinicity (see Eq. 1(b) of [26]) also results in substantial flow and dynamo action. For a rotating compressible gas, it is unlikely to derive analytical formulations that are similar to Eqs. (10)–(13), because the geometrical figure of an equilibrium becomes irregular (even non-spheroidal) [30,32, e.g.]. But it is still possible to prove, following the von Zeipel theorem, that there should not be rotational baroclinicity under the assumption of an ideal gas and that the basic reference state is adiabatic. The same conclusion can be drawn that the baroclinicity and fluid dynamics reported by Refs. [26,27] are nonphysical but a pure consequence of the choice of spherical approximation. The relevant detailed proof can be found in the Appendix.

## IV. NUMERICAL VERIFICATION

In this section, we carry out illustrative numerical simulations in order to verify the mathematical speculations drawn in Sec. III. The dimensionless equations are solved

$$\frac{\partial \boldsymbol{u}}{\partial t} + \boldsymbol{u}\cdot\nabla\boldsymbol{u} + 2\hat{z}\times\boldsymbol{u} = -\nabla\tilde{p} + St[Fr\hat{z}\times(\hat{z}\times\boldsymbol{r}) - \boldsymbol{g}_0]\tilde{T} + E\nabla^2\boldsymbol{u} + St[Fr\hat{z}\times(\hat{z}\times\boldsymbol{r}) - \boldsymbol{g}_0]T_0,$$

$$\nabla\cdot\boldsymbol{u} = 0,$$

$$Pr\left[\frac{\partial\tilde{T}}{\partial t} + \boldsymbol{u}\cdot\nabla(T_0+\tilde{T})\right] = E\nabla^2\tilde{T},$$

where the length is scaled by $R_e$; time is scaled by $\Omega^{-1}$; pressure is scaled by $\rho_0 R_e^2\Omega^2$; and temperature is scaled by $\beta R_e^2$. The three nondimensional parameters, the Ekman number $E$, the Prandtl number $Pr$ and the stratification parameter $St$ are defined as

$$E = \frac{\nu}{\Omega R_e^2}, \quad Pr = \frac{\nu}{\kappa}, \quad St = \frac{\alpha\beta\gamma R_e^2}{\Omega^2}.$$

For computational convenience, we impose the no-slip and isothermal boundary condition at the bounding surface of the oblate spheroid $\mathcal{S}$:

$$\tilde{T}(\xi = \xi_o) = 0, \quad \boldsymbol{u}(\xi = \xi_o) = 0.$$

With the above numerical settings, using a well-validated and benchmarked 3D finite-element method [33], we conduct simulations for the parameters $E = 10^{-3}$, $Pr = 7$, $St = 10^2$ and $Fr = 0.05110777$. Note that the choices of the above values of dimensionless parameters are of secondary importance for the illustrative purpose. The self-consistent geometry satisfying the Maclaurin spheroid relation Eq. (12) is marked by $e(Fr = 0.05110777) = 0.3543$ of the bounding surface $\mathcal{S}$, representing a self-consistent, nonspherical geometry of the rotating fluid. Simulations all start with zero fluid motions and adopt different geometric shapes, ranging from near-spherical to highly flattened. It is expected that zonal circulations will be driven for all cases whose geometrical shapes are inconsistent with the Maclaurin spheroid condition Eq. (12). But, according to our analysis, there ought to be no flow for the particular example, when a self-consistent geometry $e = 0.3543$ is incorporated. Figures 2 and 3 clearly verify the expectations. With the exactly self-consistent shape of the domain, no flow is driven and the model remains in hydrostatic rotational equilibrium. For inconsistent shapes of the bounding surface, however, geometrically induced baroclinicity indeed drives zonal circulations.

Note that in the calculations, the Boussinesq fluid is internally uniformly heated. In this circumstance, a self-consistent geometry results in a state free of baroclinicity, which is an exact example of the von Zeipel theorem. However, with any choice of heating other than the von Zeipel uniform heating, there will be a completely physical baroclinic flow even in the self-consistent oblate spheroidal geometry, though it will not be the same as that is given by the spherical geometry approximation.

## V. CONCLUSION AND DISCUSSION

Since the 1920s, people doubt the existence of the hydrostatic equilibrium state of a radiative star, mainly because baroclinicity seems always to appear when the star is rotating. The problem of the von Zeipel paradox [20,22] – the effect of stellar rotation may induce a torque that drives strong flow in the stably stratified radiative zone of a rotating star – was extensively studied. The previous research has mainly focused on the generation of baroclinicity due to heat source distribution that does not obey Eq. (1). This scenario is easy to understand in the case of radiative stars since realistic energy production of nuclear fusion would not spontaneously obey the uniform heat source

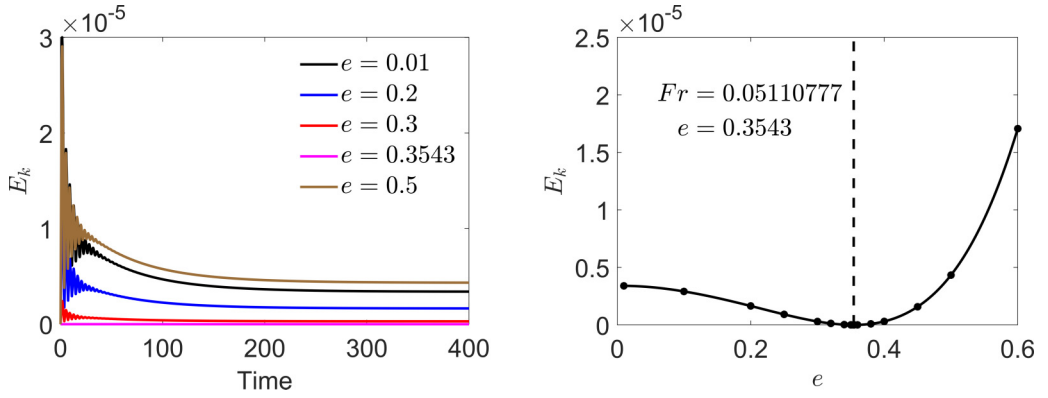


FIG. 2. Kinetic energy density of baroclinically driven flows, which is computed by the volumetric integral $Ek = \frac{1}{2\mathcal{V}} \int_{\mathcal{V}} |\boldsymbol{u}|^2 \, \mathrm{d}\mathcal{V}$. (a) shows energy curves for several typical cases of different bounding surface eccentricity values that are given in its legend. (b) plots the energy of each case when a steady zonal circulation is reached. Both panels clearly show that there is no flow for the self-consistent geometry marked by $e = 0.3543$, which exactly obeys Eq. (12) at $Fr = 0.05110777$.

requirement. In these cases there is no static equilibrium in the rotating frame, so some flow must result. This might be a differential rotation, but it could be more complex as baroclinic flows may well be unstable to Goldreich-Schubert-type instabilities and possibly others. But some very recent numerical models [25–27,34,35, e.g.] employed another source of rotational baroclinicity, which is caused by approximating the geometrical figure of a rotating stably stratified fluid body by a sphere or a spherical shell. In this paper, we see that ignoring the oblateness and assuming spherical geometry can lead to incorrect results.

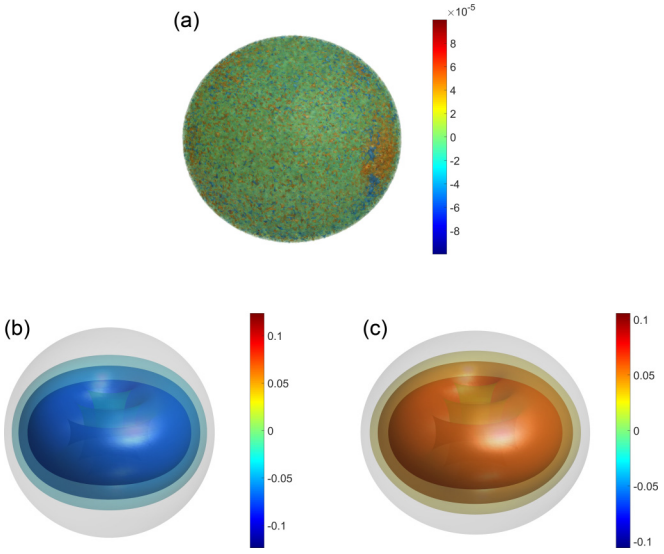


FIG. 3. Isosurfaces of the azimuthal velocity $\hat{\boldsymbol{\phi}} \cdot \boldsymbol{u}$ of baroclinically driven flows. (a) plots the case of self-consistent geometry marked by $e = 0.3543$. There is no any large scale flow but some small numerical fluctuations near zero. (b) is a near-spherical case ($e = 0.01$) whose baroclinically driven circulation is westward. (c) is an overflattened case ($e = 0.5$) whose baroclinically driven circulation is eastward. Gray partially transparent surfaces denote the bounding surfaces.

Our nonspherical model reveals that (i) the rotation-induced torque Eq. (17) reaches a maximum in spherical geometry but the spherical shape is physically unstable because of the condition Eq. (12); (ii) when a nonspherical model satisfies the equilibrium condition Eq. (12), described by the white dashed line in Fig. 1, the corresponding torque given by Eq. (17) vanishes exactly and, hence, the motionless state of static equilibrium exists in the stably stratified zone; and (iii) nonspherical geometry, although its treatment is mathematically and numerically challenging, is vital to modeling and understanding the key dynamics taking place in the stably stratified zone of a rotating star.

A motionless state of rotational equilibrium in the spheroidal geometry, given by Eq. (10)–(12), also provides a reasonably simple reference state for perturbation analysis. It opens an important new line of research in rotating astrophysical fluid dynamics, including stably stratified fluids such as precession/nutation as well as unstably stratified fluids such as thermal instabilities. In the immediately ensuing papers, nonspherical models of rapidly rotating unstable stratification are to be explored for the onset of thermal instability, convective motions, and nonlinear dynamics.

## ACKNOWLEDGMENTS

This work was supported by B-type Strategic Priority Program of the Chinese Academy of Sciences (Grant No. XDB41000000); Hong Kong-Macau-Taiwan Cooperation Funding of Shanghai Committee of Science and Technology (Grant No. 19590761300); Pre-research Project on Civil Aerospace Technologies funded by China National Space Administration (Grant No. D020303); Macau Science and Technology Development Fund (Grant No. 0005/2019/A1). The computation made use of the high-performance computing resources in the Core Facility for Advanced Research Computing at Shanghai Astronomical Observatory, Chinese Academy of Sciences.

## APPENDIX: MOTIONLESS ADIABATIC STATE OF ROTATING IDEAL GAS

Consider a rapidly rotating, self-gravitating ideal gas that is exactly in adiabatic equilibrium. The mechanical and thermal equations for pressure $p$, density $\rho$, temperature $T$ and heat source per unit mass $\varepsilon$ are

$$-\frac{\nabla p(\boldsymbol{r})}{\rho(\boldsymbol{r})}-\nabla V_g(\boldsymbol{r})-\nabla\left(-\frac{1}{2}\Omega^2 s^2\right)=\mathbf{0}, \tag{A1}$$

$$\nabla^2 V_g(\boldsymbol{r})=4\pi G\rho(\boldsymbol{r}), \tag{A2}$$

$$p(\boldsymbol{r})=K\rho(\boldsymbol{r})^{\gamma}, \tag{A3}$$

$$p(\boldsymbol{r})=\rho(\boldsymbol{r})RT(\boldsymbol{r}), \tag{A4}$$

$$\kappa\nabla^2 T(\boldsymbol{r})+\rho(\boldsymbol{r})\varepsilon(\boldsymbol{r})=0, \tag{A5}$$

where $\gamma$ is the adiabatic index of the gas, $R$ is the ideal gas constant of the gas, and $K$ is another constant that is a function of the specific entropy of the gas. Note that secular cooling effect is not considered, nuclear fusion heat generation is not considered and radiative transfer is not considered, which are consistent with the model settings in [26,27,36]. The assumptions can better describe interior state of Jupiter-like gaseous planets, rather than stars. The equations are defined in the gaseous domain whose geometrical figure is assumed to be consistent with the equilibrium, as required by von Zeipel theorem. Since we do not intend to solve the equations, the theory of figure and boundary conditions are not discussed herein.

Applying $\nabla\cdot$ to Eq. (A1), combined with Eqs. (A2) and (A3), yield

$$\gamma K\nabla\cdot(\rho^{\gamma-2}\nabla\rho)+4\pi G\rho=2\Omega^2. \tag{A6}$$

Equations (A3)–(A5) can be manipulated and reduced into

$$\varepsilon = -\frac{K\kappa(\gamma-1)}{\rho R}\nabla\cdot(\rho^{\gamma-2}\nabla\rho). \tag{A7}$$

Finally, it can be derived from Eqs. (A6) and (A7)

$$\varepsilon = \frac{4\pi G\kappa(\gamma-1)}{R\gamma}\left(1-\frac{\Omega^2}{2\pi G\rho}\right). \tag{A8}$$

According to von Zeipel theorem, hydrostatic equilibrium does exist in the corotating frame of reference because Eq. (A8) meets the requirement Eq. (1) with

$$C = \frac{4\pi G\kappa(\gamma-1)}{R\gamma}.$$


[1] S. Chandrasekhar, *Hydrodynamics and Hydrodynamic Stability* (Clarendon, Oxford, 1961)
[2] F. Busse, A simple model of convection in the Jovian atmosphere, Icarus **29**, 255 (1976).
[3] A. M. Soward, On the finite amplitude thermal instability of a rapidly rotating fluid sphere, Geophys. Astrophys. Fluid Dyn. **9**, 19 (1977).
[4] K. Zhang, On coupling between the poincaré equation and the heat equation, J. Fluid Mech. **268**, 211 (1994).
[5] K. Zhang, On coupling between the poincaré equation and the heat equation: Non-slip boundary condition, J. Fluid Mech. **284**, 239 (1995).
[6] C. A. Jones, A. W. Soward, and A. I. Mussa, The onset of thermal convection in a rapidly rotating sphere, J. Fluid Mech. **405**, 157 (2000).
[7] E. Dormy, A. M. Soward, and C. A. Jones, The onset of thermal convection in rotating spherical shells, J. Fluid Mech. **501**, 43 (1999).
[8] K. Zhang and X. Liao, A new asymptotic method for the analysis of convection in a rapidly rotating sphere, J. Fluid Mech. **518**, 319 (1999).
[9] M. Heimpel, J. Aurnou, and J. Wicht, Simulation of equatorial and high-latitude jets on jupiter in a deep convection model, Nature (London) **438**, 193 (2005).
[10] C. A. Jones, Planetary magnetic fields and fluid dynamos, Annu. Rev. Fluid Mech. **43**, 583 (2011).
[11] T. Gastine, J. Wicht, and J. Aubert, Scaling regimes in spherical shell rotating convection, J. Fluid Mech. **808**, 690 (2016).
[12] J. Sánchez, F. Garcia, and M. Net, Critical torsional modes of convection in rotating fluid spheres at high Taylor numbers, J. Fluid Mech. **791**, R1 (2016).
[13] E. J. Kaplan, N. Schaeffer, J. Vidal, and P. Cardin, Subcritical Thermal Convection of Liquid Metals in a Rapidly Rotating Sphere, Phys. Rev. Lett. **119**, 094501 (2017).
[14] B. Militzer, F. Soubiran, S. M. Wahl, and W. Hubbard, Understanding Jupiter's interior, J. Geophys. Res. Planets **121**, 1552 (2016).
[15] E. H. von Zeipel, The radiative equilibrium of a rotating system of gaseous masses, Mon. Not. R. Astron. Soc. **84**, 665 (1924).
[16] M. Rieutord and B. Dubrulle, Stellar fluid dynamics and numerical simulations: From the sun to neutron stars, EAS Publications Series **21**, 275 (2006).
[17] A. S. Eddington, Circulation currents in rotating stars, Observatory **48**, 73 (1925).
[18] H. Vogt, Zum strahlungsgleichgewicht der sterne, Astron. Nachr. **223**, 229 (1924).
[19] P. A. Sweet, The importance of rotation in stellar evolution, Mon. Not. R. Astron. Soc. **110**, 548 (1950).
[20] E. J. Öpik, Rotational currents, Mon. Not. R. Astron. Soc. **111**, 278 (1951).
[21] I. W. Roxburgh, On stellar rotataion I. The rotation of upper main-sequence stars, Mon. Not. R. Astron. Soc. **128**, 157 (1964).
[22] F. Busse, Do Eddington-sweet circulations exist? GAFD **17**, 215 (1981).

[23] H. C. Spruit and E. Knobloch, Baroclinic instability in stars, Astron. Astrophys. **132**, 89 (1984).
[24] J.-P. Zahn, Circulation and turbulence in rotating stars, Astron. Astrophys. **265**, 115 (1992).
[25] M. Rieutord, The dynamics of the radiative envelope of rapidly rotating stars I. A spherical Boussinesq model, Astron. Astrophys. **451**, 1025 (2006).
[26] R. D. Simitev and F. H. Busse, Baroclinially-driven flows and dynamo action in rotating spherical fluid shells, GAFD **111**, 369 (2017).
[27] R. D. Simitev and F. H. Busse, Flows and dynamos in a model of stellar radiative zones, J. Plasma Phys. **84**, 735840308 (2018).
[28] K. Zhang and X. Liao, *Theory and Modeling of Rotating Fluids: Convection, Inertial Waves and Precession* (Cambridge University Press, Cambridge, 2017).
[29] H. Lamb, *Hydrodynamics* (Dover Books on Physics, Dover Publications, 1945).
[30] D. Kong, K. Zhang, and G. Schubert, A fully self-consistent multi-layered model of Jupiter, Astrophys. J. **826**, 127 (2016).
[31] P. M. Morse and H. Feshbach, *Methods of Theoretical Physics* (McGraw-Hill, New York, 1953).
[32] D. Ni, Understanding saturn's interior from the Cassini grand finale gravity measurements, Astron. Astrophys. **639**, A10 (2020).
[33] K. Lam, D. Kong, and K. Zhang, Nonlinear thermal inertial waves in rotating fluid spheres, GAFD **112**, 357 (2018).
[34] F. Espinosa Lara and M. Rieutord, Self-consistent 2D models of fast-rotating early-type stars, Astron. Astrophys. **552**, A35 (2013).
[35] D. Hypolite and M. Rieutord, Dynamics of the envelope of a rapidly rotating star or giant planet in gravitational contraction, Astron. Astrophys. **572**, A15 (2014).
[36] C. Jones, P. Boronski, A. Brun, G. Glatzmaier, T. Gastine, M. Miesch, and J. Wicht, Anelastic convection-driven dynamo benchmarks, Icarus **216**, 120 (2011).